Advances of soft X-ray RIXS for studying redox reaction states in batteries

Advances of soft X-ray RIXS for studying redox reaction states in batteries

Jue Wu[1,2], Yong Yang[1,3*], Wanli Yang[2*]

[1] State Key Laboratory for Physical Chemistry of Solid Surfaces, Department of Chemistry, College of Chemistry and Chemical Engineering, Xiamen University, Xiamen 361005, China.

[2] Advanced Light Source, Lawrence Berkeley National Laboratory, One Cyclotron Road, Berkeley, California 94720, USA.

[3] School of Energy Research, Xiamen University, Xiamen 361005, China.

E-mail: yyang@xmu.edu.cn; wlyang@lbl.gov.

Abstract: Redox (reduction and oxidation) chemistry provides the fundamental basis for numerous energy-related electrochemical devices. Detecting the electrochemical redox chemistry is pivotal but challenging, because it requires independent probes of the cationic and anionic redox states at different electrochemical states. The synchrotron-based soft X-ray mapping of resonant inelastic X-ray scattering (mRIXS) has recently emerged as a powerful tool for exploring such states in electrochemical devices, especially batteries. High-efficiency and wide energy-window mRIXS covers the energy range of the absorption edge with the extra dimension of information on the emitted photon energies. In this Frontiers article, we review recent representative demonstrations on utilizing soft X-ray mRIXS for detecting the novel chemical state during electrochemical operation, and for quantifying the cationic redox reactions through inverse partial fluorescence yield analysis (mRIXS-iPFY). More importantly, the non-divalent states of oxygen in electrodes involving oxygen redox reactions could be reliably captured by mRIXS, with its reversibility quantified by the intensity variation of the characteristic mRIXS feature through a super-partial fluorescence yield analysis (mRIXS-sPFY). These recent establishments inspire future perspectives on using mRIXS for studying the complex phenomena in energy materials, with both technical and scientific challenges on RIXS theory, *in-situ/operando* experiments, and spatially resolved RIXS imaging.
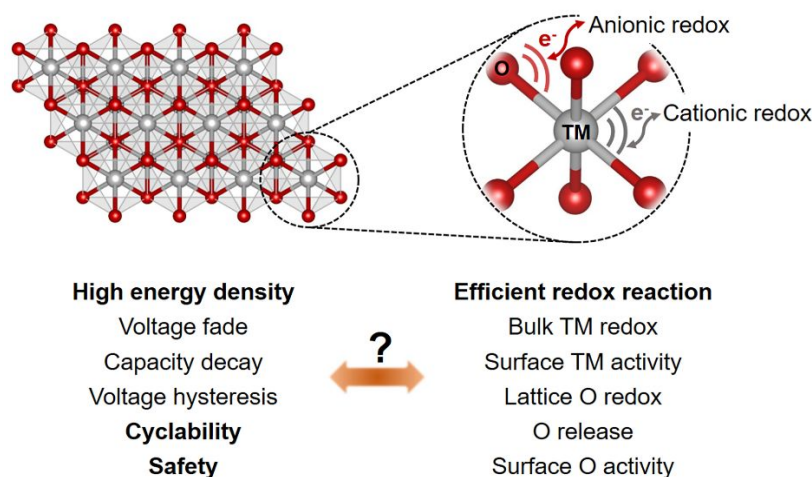
Introduction

Figure 1. Schematic of the practical challenges and cationic-anionic redox reactions in batteries. The high energy density, cyclability and safety are three important goals for battery system. These goals are closely related to the intrinsic redox reaction mechanism in battery materials and the interfaces between electrodes and electrolytes, however, the detailed relationship between them is yet to be clarified.

Electric energy storage devices based on electrochemical operations (batteries) are the key components for many modern sustainable energy applications, such as electric vehicles and green power grid. However, the demand of high-capacity high-energy batteries that could operate at high voltage under a safe and reversible condition is yet to be met[1]. In batteries, the electron charge transfer is coupled with the alkali-ion diffusion in/out of the electrodes, leading to the so-called "redox" (reduction and oxidation) reactions in the electrode materials. The redox chemistry provides the fundamental basis of electrochemical devices. Redox reaction mechanism essentially defines the capacity and stability of a battery electrode, and it may involve multiple elements in battery electrodes, especially for battery cathode. Currently, cathode has been the bottleneck of the battery capacity and practical cathode materials are typically transition metal (TM) oxides[2,3]. New cathode candidates have emerged where the theoretical or observed capacity for deintercalation exceed the capacity expected by conventional TM redox.

Naively, there are always two types of possible redox chemistry, the cationic redox and anionic redox reactions in battery electrodes. The different types of redox reactions with

different properties in amount, potential, reversibility and stability of redox reactions fundamentally define the capacity, voltage, life time, and safety, respectively[3]. In addition to the desired reversible redox reactions in batteries, undesired redox reactions, e.g., irreversible oxygen release and associated surface reactions, etc., also take place and lead to various battery problems such as voltage fade, capacity decay, voltage hysteresis and safety issues (**Figure 1**)[3]. Therefore, the in-depth detecting of an elemental and chemical resolved redox reaction mechanism becomes one of the most valuable information for understanding the operation mechanism and for optimizing the device performance.

In the conventional or commercialized Li-ion battery system, it is believed that only cationic TM reaction takes place in the practical voltage range. This often leads to a relatively stable battery operation with a typical voltage range below 4.1 V. In principle, almost all TMs could be active in the battery cathode if the cycling voltage triggers the TM redox reactions. The most typical TM elements involved in today's Li-ion batteries are Mn, Fe, Co, Ni in the cathodes, and Ti in the anodes in addition to the dominating Carbon based materials[3,4]. Experimentally, the redox states of these $3d$ TMs are more often probed by K-edge hard X-ray absorption spectroscopy (XAS). The K-edge XAS benefits from the deep penetration depth of hard X-rays, so provides true bulk probe with convenient *in-situ/operando* experiments that are almost standard these days[5,6,7]. Although K-edge XAS has been very popular in the battery field for characterizing TM redox states, the analysis often relies on the main edge shifting, which is not a directly $3d$ valence state probe and may be confusing as the edge features could vary significantly even with exactly the same oxidation state[8]. On the contrary, TM L-edge soft X-ray absorption spectroscopy (sXAS) is based on excitations directly to the valence $3d$ states, thus providing a more sensitive and direct probe of the TM oxidation states[5]. Due to the high sensitivity of TM-L sXAS to the oxidation states, sXAS spectra could be quantified directly to get almost precise numbers of the charge transfer numbers of TM redox reactions during battery operations, e.g., $Fe^{2+/3+}$, $Mn^{2+/3+/4+}$, $Ni^{2+/3+/4+}$, $Co^{3+/4+}$ and so on[9, 10, 11, 12]. The disadvantages of sXAS stem from its shallow probe depth of 10 nm or 100-200 nm in different detection modes[12]. The limitation on the sXAS probe depth complicates the *in-situ/operando* experiments[13, 14,15]. Additionally, the TM L-edge signals of the hundreds of nanometer probe depth through the so-called fluorescence yield mode suffer serious spectral lineshape distortion,

hindering its quantification. Fortunately, such a technical challenge could be addressed through the iPFY analysis, first demonstrated through commercial silicon drift detectors (SDD)[16], and recently became accessible through mRIXS with much higher energy resolution[17,18], a topic that will be elaborated later in this article.

In order to push the capacity and voltage beyond what conventional battery system could offer, recent battery researches have focused on anionic oxygen redox. The hope is to realize and utilize reversible oxygen redox reactions for accessing the high-voltage high-capacity range of the battery operation[19]. However, the oxygen redox activities often trigger detrimental effects on the battery operation, such as gas release, surface reactions, voltage drop, and sluggish kinetics. At this time, neither the fundamental mechanism nor the optimization direction of cathode materials that could enable stable and reversible oxygen redox reaction has been clarified[20]. Experimentally, detecting the lattice oxygen redox states has been a nontrivial issue. The popular X-ray photoelectron spectroscopy (XPS) has been questioned due to its surface sensitivity, and detailed analysis reveals that the peroxide assignment is actually a result of TM reduction on the surface due to oxygen loss[21]. Additionally, we have recently clarified that another popular technique of O-K sXAS is not a reliable probe of oxygen redox states due to their dominating characters from TM states in the so-called "pre-edge" range[17,22], evidenced by the significant variation in non-oxygen redox systems, such as the olivine LiFePO$_4$ and spinel Li(Ni$_{0.5}$Mn$_{1.5}$)O$_4$[10, 11, 23]. As elaborated later, such a technical challenge has been solved recently through the development of ultra-high efficiency mRIXS technique[17,18].

The purpose of this Frontier article is to highlight these recent developments pertaining to the mRIXS technique and its impacts on exploring both the cationic and anionic redox states in battery electrodes. We first introduce the basic principle and instrument requirement of mRIXS technique for studying battery materials. Next, we demonstrate the superior power offered by Mn-L and O-K mRIXS. At the end, we provide our perspectives to elaborate how mRIXS could further impact the development of next-generation batteries in different technical and scientific aspects. It is important to note that this article by no means covers all the topics of battery researches that could be tackled by soft X-ray spectroscopy, e.g., the crucial surface and interface between the electrodes and electrolyte[24,25,26]. Readers should refer to other general reviews on synchrotron-based techniques for studying batteries, especially those through the

4

conventional techniques[5]. Instead, this article focuses on the recent mRIXS developments, demonstrations, and perspectives. We also note that although mRIXS has been quickly evolving in the field of battery research, the full potential of mRIXS is yet to be explored for energy material studies; a task that is still ongoing and deserves attention of scientists in different fields of physics, chemistry and material sciences.
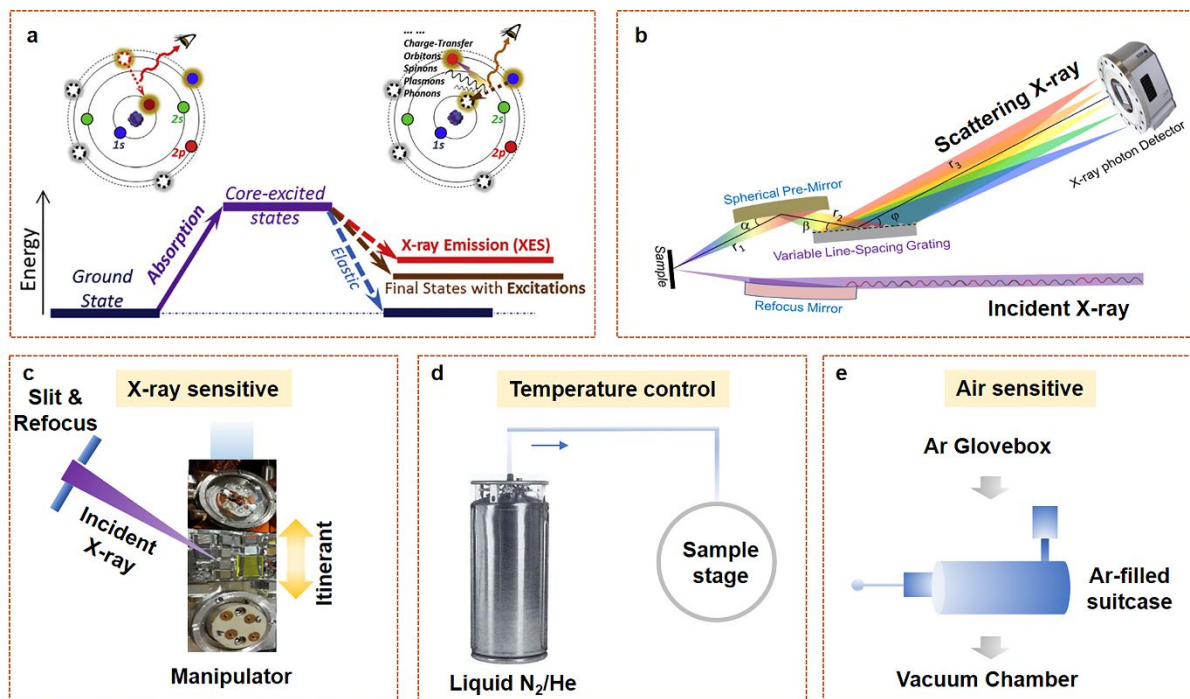
The mRIXS instrument

Figure 2. The schematic of principle and instrument for mRIXS. (a) The states involved in the RIXS process and the simplified atomic model of XES (left) and RIXS (right). Reproduced from ref. 17 with permission from the Elsevier, copyright 2018. **(b)** Schematic illustration of the optical design for a high efficiency RIXS system. Reproduced from ref. 18 with permission from the American Institute of Physics, copyright 2017. **(c)** Controlled X-ray and itinerant samples during experiments to eliminate the radiation damage effect. **(d)** Sample temperature controlled through cryogenic liquids. **(e)** Zero-air exposure sample handling through home-made transfer suitcase from the Ar-filled glovebox to soft X-ray experimental chamber.

Technically, the experimental detection of redox states in battery material is a nontrivial issue. The chemical state after electrochemical activation could be unstable in the air, especially on the surface, which requires sample handling without any exposure to the air. Secondly, the effect of X-ray irradiation could change the chemical states of the samples under investigation.

For example, it has been found that the oxidized oxygen species could be changed under X-ray irradiation, and the RIXS signals of oxidized oxygen in battery materials could decrease in intensity upon exposure to X-ray beam[27,28]. Therefore, zero-air-exposure sample handling and controlled experiments are vital for reliable analysis.

While X-ray spectroscopy has long been considered as elemental sensitive probes of the chemistry of materials, conventional techniques often show their limitations on detecting the critical chemical states in today's battery research, as briefly mentioned above. Therefore, the synchrotron-based RIXS has recently been optimized for measuring energy materials[18]. The simplified physical process for RIXS is schematically shown in **Figure 2a**. RIXS is a photon-in-photon-out (PIPO) process triggered by a core electron excitation from ground state via a tunable incident X-ray, i.e., the X-ray absorption process. The electron in excited states will then decay to fill generated core hole, which leads to different types of features in the decay process.

RIXS is a technique with very low statistics, and thus requiring very high flux of photons, which naturally triggers the technical challenges in both statistics and radiation damages due to the required high flux of X-ray photons[28]. Experimental details also involve the concerns that electrode materials are often air sensitive too. Therefore, tremendous efforts have been taken into mRIXS instrumentation to address these concerns: i) reduce the necessary X-ray radiation dose through the high efficiency spectrometer **(Figure 2b)**[18, 29] and itinerant sample manipulation during measurements (**Figure 2c**)[30]; ii) liquid nitrogen cooling to provide a low-temperature environment for certain samples, especially organic materials, to further reduce the risk of radiation damage (**Figure 2d**)[31]; iii) for air sensitive materials, during the sample preparation and transfer process, the sample will be protected in an inert argon atmosphere throughout the sample handling process via glovebox, home-made portable suitcase and load lock to avoid any air exposure (**Figure 2e**)[12].

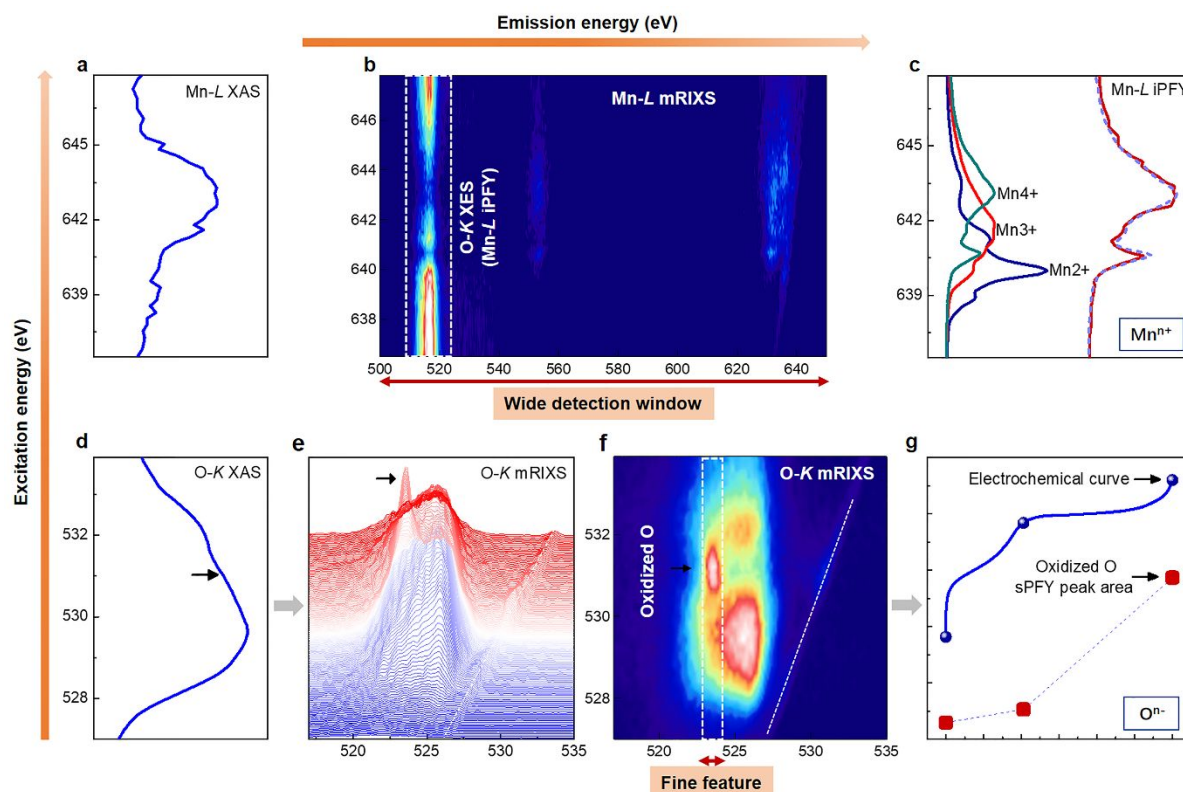**TM-*L* mRIXS**

Figure 3 Characterizations of TM and Oxygen states through mRIXS of Li$_2$MnO$_3$ and Li$_{1.2}$Ni$_{0.13}$Mn$_{0.54}$Co$_{0.13}$O$_2$, respectively. (a-c) are Mn-*L* spectroscopy of Li$_2$MnO$_3$, with signals from surface-sensitive sXAS **(a)**, bulk-sensitive Mn-*L* mRIXS **(b)** and mRIXS-iPFY **(c)**. The peak in mRIXS-iPFY spectra comes from the inverse signals of integrated O-*K* XES feature (white box) in **(b)**. **(d-g)** are oxygen state characterizations of a fully charged Li-rich Li$_{1.2}$Ni$_{0.13}$Mn$_{0.54}$Co$_{0.13}$O$_2$ electrode through O-*K* sXAS **(d)** and O-*K* mRIXS **(e, f)**. **(g)** shows the trend of the mRIXS intensity evolution of the oxidized oxygen feature through mRIXS-sPFY analysis (see text and references) by integrating the signals in the white box in (f). The trend is compared with an electrochemical cycling profile.

    In battery cathode, cationic redox reactions dominate the electrochemical operation. While we have demonstrated that, due to the high sensitivity of TM *L*-edge to the valence 3*d* states, *L*-edge sXAS could be utilized for quantitative analysis of TM states[32], the sXAS for such an analysis is limited to surface signals due to the serious distortion of the lineshape of the PIPO channel with bulk signals (**Figure 3a**). By extracting iPFY from the mRIXS result, a direct oxidation state quantification of bulk Mn is realized by Mn-*L* mRIXS-iPFY[18]. **Figure 3b** presents a typical Mn-*L* mRIXS data of a battery cathode, Li-rich Li$_2$MnO$_3$. It is a two-

dimensional map with information including excitation energy, emission energy and emission peak intensity. The Mn-L mRIXS-iPFY spectra could be gained by integrating the O-K XES emission energy area (white dashed square in **Figure 3b**) of the Mn-L mRIXS map then inverse the integrated intensity. **Figure 3c** displays the mRIXS-iPFY of a model system, Li_2MnO_3. Although conventional Mn fluorescence yield signals always suffer serious lineshape distortion[16], hindering its quantitative analysis, the extracted mRIXS-iPFY spectrum displays almost exactly the same Mn^{4+} lineshape as that from the surface sensitive electron yield signals (dashed line and reference spectra) without any lineshape distortion.

In battery materials, Mn is one of the most important TM elements, owing to its low cost, high abundance, and low toxicity. However, quantifying the Mn oxidation states has been challenging with conventional spectroscopic techniques, including XPS and hard X-ray Mn-K spectroscopy[8]. The combined sXAS surface signals through the electron yield channel and mRIXS-iPFY bulk data characterizes quantitatively the Mn oxidation state evolution on both the electrode surface and in the bulk upon electrochemical states[33].

Additionally, mRIXS data provides a new dimension of information along the emission energy that is completely missing in conventional sXAS spectra. This leads to the improved chemical sensitivity to novel oxidation state that cannot be clearly probed through conventional spectroscopy. For example, recent investigation in prussian blue analogs, $Na_{1.24}Mn[Mn(CN)_6]\cdot2.1H_2O$ through Mn-L mRIXS directly reveals the unusual monovalent manganese in the charged anode (**Figure 4d**)[34]. This is the first time that a low spin $3d^6$ system, Mn^{1+}, is directly fingerprinted based on the power of mRIXS. In general, mRIXS has been developed as a highly valuable tool for systematically exploring the low-energy charge, spin, orbital and lattice excitations, which could be further extended in energy material[35].

These demonstrations highlight the unique ability of TM-L mRIXS data in revealing TM redox contribution for electrochemistry process. The results derived from TM-L mRIXS could either provide a quantitative evaluation of the bulk TM chemical states or detect novel chemical states in the battery systems that are hard to be sensed through other characterizations.

O-K mRIXS

A more important application of mRIXS studies on battery materials is to characterize the oxygen redox reaction in oxide-based battery cathodes. The oxygen activity usually consists

of different types of oxygen-involved reactions, such as gas release, radical oxygen evolution and surface reaction[36]. The mRIXS under the ultra-high vacuum condition naturally rules out the signals of the gas species, and distinguishes lattice oxygen redox reactions from other released oxygen. Compared with conventional O-K sXAS spectra (**Figure 3d**), mRIXS further resolves the emission energy of the signals. It has been found that a striking feature at around 523.7 eV emission energy and around 531.0 excitation energy appears in mRIXS (black arrow in **Figure 3e, 3f**) that is buried in the "pre-edge" of sXAS spectra (**Figure 3d**). Indeed, we have clarified that the O-K sXAS pre-edge is dominated by the TM character through strong hybridization effects, thus is not a reliable probe of oxygen redox states in oxide based battery electrodes[17,22]. Such a feature was observed through high-efficiency gas phase mRIXS experiments of various oxidized oxygen species, such as Li_2O_2 and O_2[37, 38]. For battery materials, this fingerprint of the oxidized oxygen has been confirmed in Li-rich layered cathode (**Figure 4c**)[39-42], Li-rich disordered rocksalt electrodes[43-46], conventional Li-ion battery electrode materials[47-50], and Na-ion battery materials[33,51,52]. However, it is important to note that the fundamental mechanism of the oxygen redox reaction is still under active debates, and these mRIXS results have yet to be fully understood. A recent comparison on the mRIXS data for $O^-(Li_2O_2)$, $O^0(O_2)$, $O^{2-}(CO_2)$ and battery cathode oxide reveals that the oxidized oxygen state in battery material is beyond a simple molecular configuration of either the peroxide or oxygen gas type, and may be even different among different cathode materials[37].

For practical applications of oxygen redox reactions, the kinetics and the reversibility are always the most serious concerns[20]. By virtue of the high sensitivity of mRIXS, the reversibility of oxygen redox reactions could be detected by tracking the evolution of the corresponding mRIXS feature intensity upon electrochemical cycling, which could be quantified through mRIXS-sPFY[33]. During electrochemical operation, the intensity of the oxidized oxygen feature evolves systematically with the electrochemical charge-discharge process, indicating the reversibility of the oxygen redox reaction[30]. As shown in **Figure 3f**, the one-dimension sPFY spectra is gained via extracting and integrating the 523.7 eV emission energy feature (range from 523.0 eV to 524.5 eV emission energy). The reversibility of oxygen redox could then be gained via intensity comparisons between the charge and discharge states (**Figure 3g**). For example, $Na_{2/3}Mg_{1/3}Mn_{2/3}O_2$ has been confirmed delivering 79% reversible

lattice oxygen redox in the initial cycle and 87% sustained after 100 cycles via O-K mRIXS-sPFY analysis (**Figure 4f**)[33].

Additionally, the mRIXS presents its superior sensitivity for probing the subtle change in chemical environment. The oxygen redox reaction behavior has been proposed being sensitive to the chemical environment, such as the local structure, surrounding atoms and interatomic interaction[53,54]. However, detecting such a subtle change of the chemical environment is extremely difficult because the critical signals are usually buried in the strong background. Recently, by employing mRIXS, an intriguing interaction between the protons and oxygen is revealed in acid-treated Li_2MnO_3 battery materials[31]. As shown in **Figure 4e**, compared with the pristine and reference samples, not only a reversible oxygen redox feature, but also a moderate coupling between lattice oxygen and protons through a beneficial inductive effect is directly observed through O-K mRIXS in treated sample. The interaction probe provides valuable information on the detailed configuration in cathode oxide, and such findings from mRIXS open up new opportunities for studying the electrochemical energy storage material with subtle chemical variations. As another example, the local electronic structure of aqueous potassium chloride solution can be studied by RIXS to monitor the effect of the ion solvation on the hydrogen-bond network of liquid water. The significant change in the O K-edge RIXS spectra are observed upon KCl concentration change, which can be attributed to the modifications in the proton dynamics, caused by a specific coordination structure around the salt ions[55]. Detecting these subtle chemical variations in battery system, e.g., chemistry in electrodes and solvation shells in electrolyte, has been a grand challenge for understanding and improving a battery system, mRIXS has now been demonstrated as a powerful tool to provide unprecedented information on these hard topics.
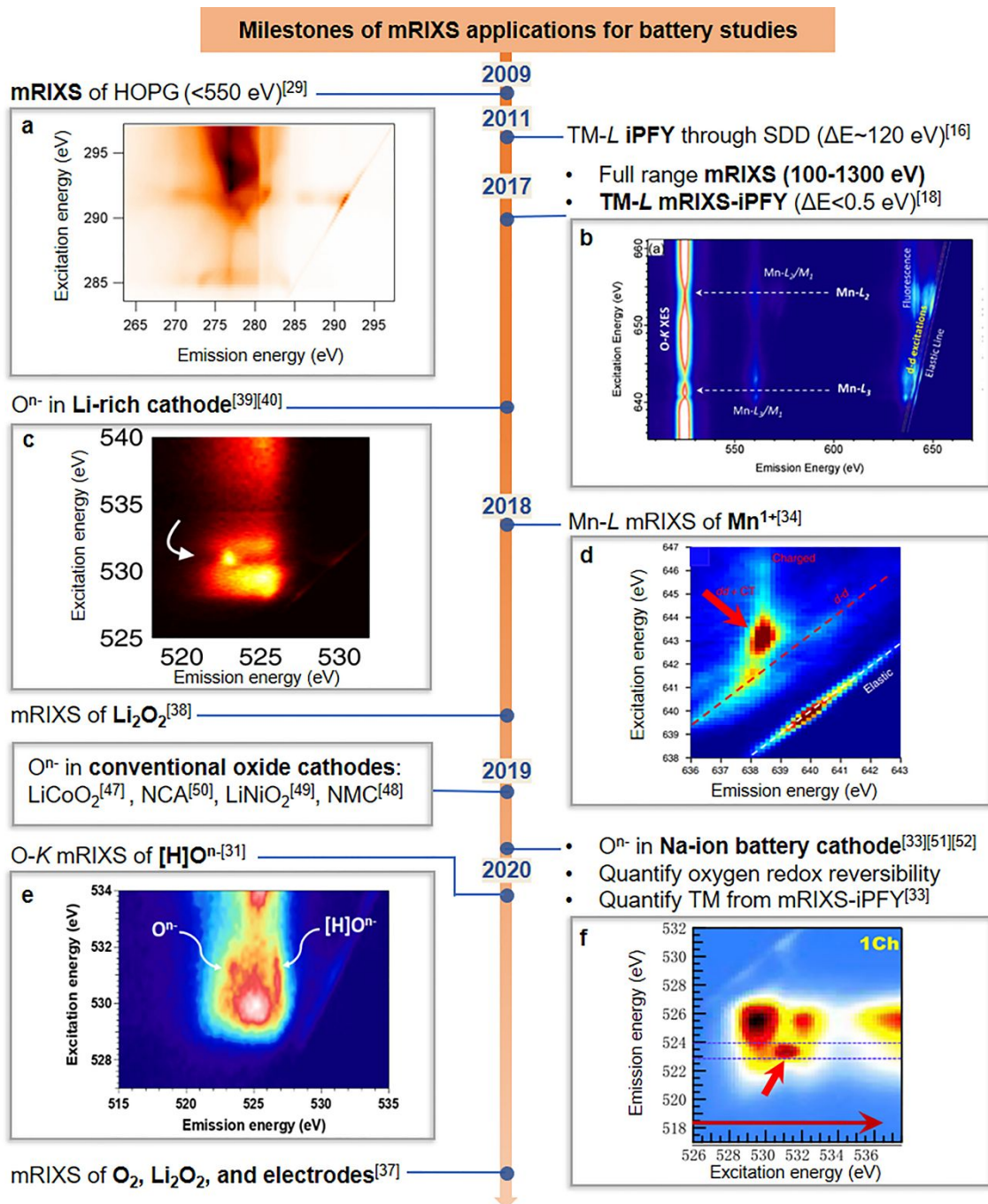
Conclusions and outlook

Figure 4. Milestones in the establishment of mRIXS as a unique tool in battery research.
(a) A high-efficiency mRIXS system was developed in low-energy range in 2009. Reproduced from ref. 29 with permission from the American Institute of Physics, copyright 2009. **(b)** full soft X-ray energy range mRIXS system was commissioned in 2017, covering *L*-edges of all *3d* TMs. A demonstration of mRIXS-iPFY of Mn-*L* is shown here. Reproduced from ref. 18 with permission from the American Institute of Physics, copyright 2017. Representative examples are selected to cover different aspects of mRIXS applications in batteries: **(c)** mRIXS signature of the oxygen redox states in Li-rich electrodes, reproduced from ref. 39 with permission from the Springer Nature, copyright 2017; **(d)** excitation features in mRIXS of TMs define novel TM states, reproduced from ref. 34 with permission from the Springer Nature, copyright 2018; **(e)** mRIXS fingerprints the subtle chemical change of O affected by an inductive effect from a

proton in the vicinity, reproduced from ref. 31 with permission from the American Chemical Society, copyright 2020; **(f)** well-defined oxygen redox mRIXS features in Na-ion battery electrode quantify the reversibility and cyclability of oxygen redox reactions. Reproduced from ref. 33 with permission from the Elsevier, copyright 2018.

A battery is a complex system that is yet to be comprehensively understood. The redox states involved in battery operation are one of the keys in chemistry of the fundamental mechanism and practical optimizations. As illustrated above, mRIXS technique has become pivotal to reveal and characterize the redox states in both the cations and anions, sometimes as almost the only choice for detecting unconventional chemical states in batteries. **Figure 4** presents the key milestones in the development of mRIXS in the past decades, starting from the development of a high-efficiency spectrograph covering low photo energy range and the demonstration of a fast mRIXS collection of HOPG (**Figure 4a**)[29]. In 2017, ultra-high efficiency spectrograph were developed covering the full soft X-ray energy range, especially for collecting TM-*L* mRIXS-iPFY(**Figure 4b**)[18], which turns out to be a valuable tool for quantitative analysis of the bulk TM states, as elaborated in this work. Here, we highlight that mRIXS enables the mRIXS-iPFY detection channel with superior energy resolution for quantitative measurements of the TM redox reactions[33]. The TM-*L* mRIXS features also provide much more sensitive detection of unconventional state, e.g., Mn^{1+}, that cannot be sensed through any conventional technique[34]. More importantly, the improved chemical sensitivity through the new dimension of information along emission energy could differentiate the intrinsic oxygen redox state from the dominating signals from TM-O hybridization.

We note that the power of mRIXS has not been explored and capitalized on to its full potential, e.g., the recent mRIXS detection of the subtle chemical changes of oxygen affected by only an inductive effect opens up new opportunities of using mRIXS to study polyanionic frameworks such as phosphates, silicates, and sulfates[31]. With new capabilities of mRIXS being continuously explored, the employment of mRIXS for energy material researches will becomes more and more indispensable.

Other than the advances in mRIXS techniques and experimental findings, we have to realize that fully understanding the striking mRIXS features in energy materials remains a grand challenge for spectroscopy physics, especially in theory. For example, although the

oxygen redox feature has been found in non-divalent oxygen references like peroxide and O_2[38], detailed comparison between them shows that the features of TM oxide based electrodes are different from those reference compounds[37], indicating the fundamental form of the oxidized oxygen may not be simply a molecular configuration. It is obviously that theoretical interpretation of the mRIXS feature of TM oxide electrode holds the promise to uncover the mystery of the oxidized oxygen state in the oxygen redox system. We note that calculations of sXAS results could reach a fairly quantitative level through recent developments[56,57]; however, RIXS calculations of the oxide-based complex cathode system remains challenging and deserves further collaborative works between theoretical physics, spectroscopy, and material sciences.

The battery research has also evolved into extensive studies of solid-state batteries in recent years, due to the benefit of solid-state electrolyte for potentially working with high capacity electrode, e.g., Li metal, under safe operations. However, many scientific and technical challenges remain[58]. The mRIXS technique, with its superior chemical sensitivity beyond conventional spectroscopic tools in both TM and O, as demonstrated here, provides unique opportunities for studying the interface and high capacity electrode materials. On the other hand, the solid-state electrolyte is naturally compatible with the ultra-high vacuum that is required for soft X-ray spectroscopy experiments. Typical *in-situ* soft X-ray experiments require sophisticated model cell systems that could only mimic the electrochemical operation with complicated signals especially for O and C[13, 14]. The solid-state battery setups could enable straightforward *in-situ* setups for truly real-world experiments[14, 17]. This mutual benefit will further advance both the mRIXS technical developments and its scientific impacts.

Last but not the least, RIXS is principally a photon-hungry experiment, which often triggers the concern of radiation damage, especially for the unconventional chemical states that are often unstable[28]. We note this problem will become more serious when the light sources evolve into the next generation of diffraction limited rings. Obviously, merely improving the incident X-ray beam will not solve this problem. Enhancing the detecting efficiency with relatively broadened beam size has been demonstrated to be an effective solution, which requires continuous innovations in spectrometer designs that not only focuses on resolution but also throughput. Unfortunately, the broadened beam size casts a natural limitation on the spatial

resolution of the mRIXS technique. Such a dilemma could only be resolved if mRIXS could be performed in an imaging mode without the need of beam focusing. This formidable challenge has recently been cracked through a spectrometer based on Wolter-mirror designs with other technical advances, through which, a spatial resolution of 100 nm with a time resolution of 1 ns could be achieved[59]. We expect that, coupled with the new-generation diffraction-limited light sources, further developments of RIXS technique into the spatial and temporal domains, coupled with its superior elemental and chemical sensitivities, will further revolutionize the characterizations of energy materials in a vast field beyond battery research.

Conflicts of interest

There are no conflicts to declare.

Acknowledgements

References

1.   J.-M. Tarascon and M. Armand, *Nature*, 2011, **414**, 359-367.

2.   M. S. Whittingham, *Chem. Rev.*, 2004, **104**, 4271-4302.

3.   J. B. Goodenough and Y. Kim, *Chem. Mater.*, 2010, **22**, 587-603.

4.   B. L. Ellis, K. T. Lee and L. F. Nazar, *Chem Mater*, 2010, **22**, 691-714.

5.   F. Lin, Y. Liu, X. Yu, L. Cheng, A. Singer, O. G. Shpyrko, H. L. Xin, N. Tamura, C. Tian and

        T.-C. Weng, *Chem. Rev.*, 2017, **117**, 13123-13186.

6.   X. Yu, Y. Lyu, L. Gu, H. Wu, S.-M. Bak, Y. Zhou, K. Amine, S. N. Ehrlich, H. Li, K.-W. Nam and X.-Q. Yang, *Adv. Energy Mater.*, 2014, **4**, 1300950.

7.   Y.-N. Zhou, J.-L. Yue, E. Hu, H. Li, L. Gu, K.-W. Nam, S.-M. Bak, X. Yu, J. Liu, J. Bai, E. Dooryhee, Z.-W. Fu and X.-Q. Yang, *Adv. Energy Mater.*, 2016, **6**, 1600597.

8.   A. Manceau, M. A. Marcus and S. Grangeon, *Am. Mineral.*, 2012, **97**, 816-827.

9.   X. Liu, J. Liu, R. Qiao, Y. Yu, H. Li, L. Suo, Y. S. Hu, Y. D. Chuang, G. Shu, F. Chou, T. C. Weng, D. Nordlund, D. Sokaras, Y. J. Wang, H. Lin, B. Barbiellini, A. Bansil, X. Song, Z. Liu, S. Yan, G. Liu, S. Qiao, T. J. Richardson, D. Prendergast, Z. Hussain, F. M. de Groot and W. Yang, *J. Am. Chem. Soc.*, 2012, **134**, 13708-13715.

10.   R. Qiao, Y. Wang, P. Olalde-Velasco, H. Li, Y.-S. Hu and W. Yang, *J. Power Sources*, 2015, **273**, 1120-1126.

11.   R. Qiao, L. A. Wray, J.-H. Kim, N. P. W. Pieczonka, S. J. Harris and W. Yang, *J. Phys. Chem. C*, 2015, **119**, 27228-27233.

12.   W. Yang, X. Liu, R. Qiao, P. Olalde-Velasco, J. D. Spear, L. Roseguo, J. X. Pepper, J. D. Denlinger and Z. Hussain, *J. Electron Spectrosc. Relat. Phenom.*, 2013, **190**, 64-74.

13.   J. Guo, *J. Electron Spectrosc. Relat. Phenom.*, 2013, **188**, 71-78.

14.   X. Liu, W. Yang and Z. Liu, *Adv Mater*, 2014, **26**, 7710-7729.

15.   X. Liu, D. Wang, G. Liu, V. Srinivasan, Z. Liu, Z. Hussain and W. Yang, *Nat. Commun.*, 2013, **4**, 2568.

16.   A. J. Achkar, T. Z. Regier, H. Wadati, Y. J. Kim, H. Zhang and D. G. Hawthorn, *Phys Rev B*, 2011, **83**, 081106.

17.   W. Yang and T. P. Devereaux, *J. Power Sources*, 2018, **389**, 188-197.

18.   R. Qiao, Q. Li, Z. Zhuo, S. Sallis, O. Fuchs, M. Blum, L. Weinhardt, C. Heske, J. Pepper, M.

Jones, A. Brown, A. Spucces, K. Chow, B. Smith, P. A. Glans, Y. Chen, S. Yan, F. Pan, L. F.

Piper, J. Denlinger, J. Guo, Z. Hussain, Y. D. Chuang and W. Yang, *Rev. Sci. Instrum.*, 2017,

88, 033106.

19.   A. Grimaud, W. Hong, Y. Shao-Horn and J.-M. Tarascon, *Nat. Mater.*, 2016, **15**, 121-126.

20.   G. Assat and J.-M. Tarascon, *Nature Energy*, 2018, **3**, 373-386.

21.   Z. W. Lebens-Higgins, H. Chung, M. J. Zuba, J. Rana, Y. Li, N. V. Faenza, N. Pereira, B. D.

McCloskey, F. Rodolakis, W. Yang, M. S. Whittingham, G. G. Amatucci, Y. S. Meng, T.-L. Lee

and L. F. J. Piper, *J. Phys. Chem. Lett.*, 2020, **11**, 2106-2112.

22.   Q. Ruimin, R. Subhayan, Z. Zengqing, L. Qinghao, L. Yingchun, K. Jung-Hyun, L. Jun, L.

Eungje, P. Bryant J, G. Jinghua, Y. Shishen, H. Yongsheng, L. Hong, P. David and Y. Wanli,

ChemRxiv, 2019, DOI: 10.26434/chemrxiv.11416374.v2.

23.   X. Liu, Y. J. Wang, B. Barbiellini, H. Hafiz, S. Basak, J. Liu, T. Richardson, G. Shu, F. Chou

and T.-C. Weng, *Phys. Chem. Chem. Phys.*, 2015, **17**, 26369-26377.

24.   Z. Q. Zhuo, P. Lu, C. Delacourt, R. M. Qiao, K. Xu, F. Pan, S. J. Harris and W. L. Yang, *Chem.*
Commun., 2018, **54**, 814-817.

25.   R. Qiao, I. T. Lucas, A. Karim, J. Syzdek, X. Liu, W. Chen, K. Persson, R. Kostecki and W.

Yang, *Advanced Materials Interfaces*, 2014, **1**, 1300115.

26.   Q. H. Li, S. S. Yan and W. L. Yang, *J. Chem. Phys.*, 2020, **152**, 140901.

27.   R. Qiao, Y. D. Chuang, S. Yan and W. Yang, *PLoS One*, 2012, **7**, e49182.

28.   Z. W. Lebens-Higgins, J. Vinckeviciute, J. Wu, N. V. Faenza, Y. Li, S. Sallis, N. Pereira, Y. S.

Meng, G. G. Amatucci and A. V. Der Ven, *J. Phys. Chem. C*, 2019, **123**, 13201-13207.

29. O. Fuchs, L. Weinhardt, M. Blum, M. Weigand, E. Umbach, M. Baer, C. Heske, J. Denlinger, Y. D. Chuang, W. McKinney, Z. Hussain, E. Gullikson, M. Jones, P. Batson, B. Nelles and R. Follath, *Rev. Sci. Instrum.*, 2009, **80**, 063103.

30. J. Wu, Q. Li, S. Sallis, Z. Zhuo, W. E. Gent, W. C. Chueh, S. Yan, Y.-d. Chuang and W. Yang, *Condens. Matter*, 2019, **4**, 5.

31. J. Wu, X. Zhang, S. Zheng, H. Liu, J. Wu, R. Fu, Y. Li, Y. Xiang, R. Liu, W. Zuo, Z. Cui, Q. Wu, S. Wu, Z. Chen, P. Liu, W. Yang and Y. Yang, *ACS Appl. Mater. Interfaces*, 2020, **12**, 7277-7284.

32. Q. Li, R. Qiao, L. A. Wray, J. Chen, Z. Zhuo, Y. Chen, S. Yan, F. Pan, Z. Hussain and W. Yang, *J. Phys. D: Appl. Phys.*, 2016, **49**, 413003.

33. K. Dai, J. Wu, Z. Zhuo, Q. Li, S. Sallis, J. Mao, G. Ai, C. Sun, Z. Li, W. E. Gent, W. C. Chueh, Y.-d. Chuang, R. Zeng, Z.-x. Shen, F. Pan, S. Yan, L. F. J. Piper, Z. Hussain, G. Liu and W. Yang, *Joule*, 2019, **3**, 518-541.

34. A. Firouzi, R. Qiao, S. Motallebi, C. W. Valencia, H. S. Israel, M. Fujimoto, L. A. Wray, Y. D. Chuang, W. Yang and C. D. Wessells, *Nat Commun*, 2018, **9**, 861.

35. L. J. Ament, M. Van Veenendaal, T. P. Devereaux, J. P. Hill and J. Van Den Brink, *Rev. Mod. Phys.*, 2011, **83**, 705.

36. W. Yang, *Nature Energy*, 2018, **3**, 619-620.

37. Z. Zhuo, Y.-S. Liu, J. Guo, Y.-d. Chuang, F. Pan and W. Yang, *J. Phys. Chem. Lett.*, 2020, **11**, 2618-2623.

38. Z. Zhuo, C. D. Pemmaraju, J. Vinson, C. Jia, B. Moritz, I. Lee, S. Sallis, Q. Li, J. Wu, K. Dai, Y. D. Chuang, Z. Hussain, F. Pan, T. P. Devereaux and W. Yang, *J. Phys. Chem. Lett.*, 2018, **9**,

6378-6384.

39. W. E. Gent, K. Lim, Y. Liang, Q. Li, T. Barnes, S. J. Ahn, K. H. Stone, M. McIntire, J. Hong, J. H. Song, Y. Li, A. Mehta, S. Ermon, T. Tyliszczak, D. Kilcoyne, D. Vine, J. H. Park, S. K. Doo, M. F. Toney, W. Yang, D. Prendergast and W. C. Chueh, *Nat Commun*, 2017, **8**, 2091.

40. J. Xu, M. Sun, R. Qiao, S. E. Renfrew, L. Ma, T. Wu, S. Hwang, D. Nordlund, D. Su, K. Amine, J. Lu, B. D. McCloskey, W. Yang and W. Tong, *Nat Commun*, 2018, **9**, 947.

41. S. Ramakrishnan, B. Park, J. Wu, W. Yang and B. D. McCloskey, *J. Am. Chem. Soc.*, 2020, **142**, 8522-8531.

42. J. Wu, Q. Li, S. Sallis, Z. Zhuo, W. Gent, W. Chueh, S. Yan, Y.-d. Chuang and W. Yang, *Condensed Matter*, 2019, **4**, 5.

43. E. Zhao, Q. Li, F. Meng, J. Liu, J. Wang, L. He, Z. Jiang, Q. Zhang, X. Yu, L. Gu, W. Yang, H. Li, F. Wang and X. Huang, *Angew. Chem., Int. Ed.*, 2019, **58**, 4323-4327.

44. H. Ji, J. Wu, Z. Cai, J. Liu, D.-H. Kwon, H. Kim, A. Urban, J. K. Papp, E. Foley, Y. Tian, M. Balasubramanian, H. Kim, R. J. Clément, B. D. McCloskey, W. Yang and G. Ceder, *Nature Energy*, 2020, **5**, 213-221.

45. D. Chen, J. Wu, J. K. Papp, B. D. McCloskey, W. Yang and G. Chen, *Small*, 2020, DOI: 10.1002/smll.202000656.

46. M. Luo, S. Zheng, J. Wu, K. Zhou, M. Feng, H. He, R. Liu, G. Zhao, S. Chen, W. Yang, Z. Peng, Q. Wu and Y. Yang, *J. Mater. Chem. A*, 2020, **8**, 5115-5127.

47. J.-N. Zhang, Q. Li, C. Ouyang, X. Yu, M. Ge, X. Huang, E. Hu, C. Ma, S. Li, R. Xiao, W. Yang, Y. Chu, Y. Liu, H. Yu, X.-Q. Yang, X. Huang, L. Chen and H. Li, *Nature Energy*, 2019, **4**, 594-603.

48.   G.-H. Lee, J. Wu, D. Kim, K. Cho, M. Cho, W. Yang and Y. Kang, *Angew. Chem., Int. Ed.*, 2020, **59**, 8681–8688.

49.   N. Li, S. Sallis, J. K. Papp, J. Wei, B. D. McCloskey, W. Yang and W. Tong, *ACS Energy Lett.*, 2019, **4**, 2836-2842.

50.   Z. W. Lebens-Higgins, N. V. Faenza, M. D. Radin, H. Liu, S. Sallis, J. Rana, J. Vinckeviciute, P. J. Reeves, M. J. Zuba, F. Badway, N. Pereira, K. W. Chapman, T.-L. Lee, T. Wu, C. P. Grey, B. C. Melot, A. Van Der Ven, G. G. Amatucci, W. Yang and L. F. J. Piper, *Mater. Horiz.*, 2019, **6**, 2112-2123.

51.   J. Wu, Z. Zhuo, X. Rong, K. Dai, Z. Lebens-Higgins, S. Sallis, F. Pan, L. F. J. Piper, G. Liu, Y.-d. Chuang, Z. Hussain, Q. Li, R. Zeng, Z.-x. Shen and W. Yang, *Science Advances*, 2020, **6**, eaaw3871.

52.   K. Dai, J. Mao, Z. Zhuo, Y. Feng, W. Mao, G. Ai, F. Pan, Y.-d. Chuang, G. Liu and W. Yang, *Nano Energy*, 2020, **74**, 104831.

53.   D.-H. Seo, J. Lee, A. Urban, R. Malik, S. Kang and G. Ceder, *Nat. Chem.*, 2016, **8**, 692.

54.   N. Yabuuchi, M. Nakayama, M. Takeuchi, S. Komaba, Y. Hashimoto, T. Mukai, H. Shiiba, K. Sato, Y. Kobayashi and A. Nakao, *Nat. Commun.*, 2016, **7**, 1-10.

55.   Y. L. Jeyachandran, F. Meyer, S. Nagarajan, A. Benkert, M. Baer, M. Blum, W. Yang, F. Reinert, C. Heske, L. Weinhardt and M. Zharnikov, *J. Phys. Chem. Lett.*, 2014, **5**, 4143-4148.

56.   Y. Liang, J. Vinson, S. Pemmaraju, W. S. Drisdell, E. L. Shirley and D. Prendergast, *Phys. Rev. Lett.*, 2017, **118**, 096402.

57.   G. J. Paez, C. N. Singh, M. J. Wahila, K. E. Tirpak, N. F. Quackenbush, S. Sallis, H. Paik, Y. Liang, D. G. Schlom, T.-L. Lee, C. Schlueter, W.-C. Lee and L. F. J. Piper, *Phys. Rev. Lett.*,

2020, **124**, 196402.

58.   Y. Xiang, X. Li, Y. Cheng, X. Sun and Y. Yang, *Mater. Today*, 2020, **36**, 139-157.

59.   Y.-D. Chuang, X. Feng, P.-A. Glans-Suzuki, W. Yang, H. Padmore and J. Guo, *J. Synchrotron Rad.*, 2020, **27**, 695-707.
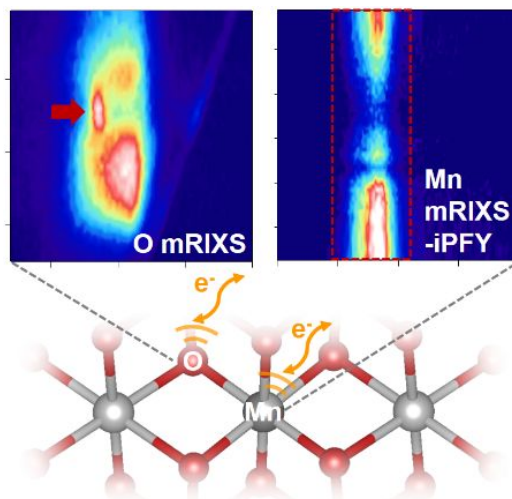
High-efficiency mapping of resonant inelastic X-ray scattering (mRIXS) for detecting and quantifying both cationic and anionic redox states in batteries.